Complex Mare Deposits Revealed by CE-2 CELMS Data in Mare Nubium

Zhiguo Meng, *Member, IEEE*, Shengbo Chen, *Member, IEEE*, Yongzhi Wang, Weiming Cheng, Shuanggen Jin, *Member, IEEE*, Zhanchuan Cai, *Senior Member, IEEE*, and Shuo Hu

***Abstract*—The study of mare basalts in microwave range will be of great significance to better understand the basaltic units with complex surface contaminations, particularly in Mare Nubium. In this article, the China Chang′E-2 Lunar Microwave Sounder data and the generated normalized brightness temperature (nTB) and brightness temperature difference (dTB) maps are employed to evaluate the basaltic units in Mare Nubium. The results are as follows. First, two regions with hot anomaly are found, which is likely brought by the high substrate temperature. The anomaly in central Nubium is extensive in range and high in intensity. Second, the nTB and dTB performances can pursue the mare deposits contaminated by the impact ejecta, which reveals special mare basalt with the thin layer in the southeastern part of Mare Nubium. Third, the nTB and dTB maps indicate the complexity of the mare deposits in Mare Nubium. Fourth, the cold dTB anomaly in the western part is proposed as the floor deposits produced during the formation of the Nubium basin. These unusual findings will be of fundamental significance to better understand the basaltic volcanism and the thermal evolution of the Moon.**

Manuscript received February 29, 2020; revised May 6, 2020; accepted May 14, 2020. Date of publication May 26, 2020; date of current version June 4, 2020. This work was supported in part by the B-type Strategic Priority Program of the Chinese Academy of Sciences under Grant XDB41000000, in part by a grant from the State Key Laboratory of Resources and Environmental Information System, in part by the Fundamental Research Funds for the Central Universities, in part by the opening fund of State Key Laboratory of Lunar and Planetary Sciences (Macau University of Science and Technology) (Macau FDCT Grant 119/2017/A3), in part by the Science and Technology Development Fund of Macau under Grant 0012/2018/A1, and in part by the National Key R&D Program of China under Grant 2017YFC0602203. *(Corresponding author: Yongzhi Wang.)*

Zhiguo Meng is with the College of Geoexploration Science and Technology, Jilin University, Changchun 130026, China, with the State Key Laboratory of Resources and Environmental Information System, Institute of Geographic Sciences and Natural Resources Research, CAS, Beijing 100101, China, with the State Key Laboratory of Lunar and Planetary Sciences, Macau University of Science and Technology, 999078, Macau, and also with the Institute of National Development and Security Studies, Jilin University, Changchun 130012, China (e-mail: mengzg@jlu.edu.cn).

Shengbo Chen, Yongzhi Wang, and Shuo Hu are with the College of Geoexploration Science and Technology, Jilin University, Changchun 130026, China (e-mail: chensb@jlu.edu.cn; iamwangyongzhi@126.com; whosure@126.com).

Weiming Cheng is with the State Key Laboratory of Resources and Environmental Information System, Institute of Geographic Sciences and Natural Resources Research, CAS, Beijing 100101, China (e-mail: chengwm@lreis.ac.cn).

Zhanchuan Cai is with the State Key Laboratory of Lunar and Planetary Sciences, Macau University of Science and Technology, 999078, Macau, and also with the Faculty of Information Technology, Macau University of Science and Technology, 999078, Macau (e-mail: zccai@must.edu.mo).

Shuanggen Jin is with the Key Laboratory of Planetary Sciences, Shanghai Astronomical Observatory, CAS, Shanghai 200030, China, and also with the School of Remote Sensing and Geomatics Engineering, Nanjing University of Information Science and Technology, Nanjing 210044, China (e-mail: sgjin@shao.ac.cn).

Digital Object Identifier 10.1109/JSTARS.2020.2996266

***Index Terms*—Basaltic unit, Chang′E Lunar Microwave Sounder (CELMS) data, Mare Nubium, Microwave propagation, Microwave thermal emission, Remote sensing.**

I. Introduction

MARE Nubium, centered at 20.59°S and 17.29°W, has a diameter of 714.5 km USGS[1], and is one of the most ancient circular impact basins on the Moon [see Fig. 1(a)]. The lava flow units in Mare Nubium have a range of ages from Imbrian to Eratosthenian period (2.8–3.8 Ga) [1], [2]. In this article, the China Chang'E Lunar Microwave Sounder (CELMS) data from Chang′E-2 (CE-2) lunar orbiter are used to probe the microwave thermal emission features of the region around Mare Nubium. The thermal study of the regions in microwave wavelengths can be used to acquire valuable information about the volcanic history of the Moon compared to the optical and earth-based radar data.

Until now, visible and infrared data were widely used to evaluate the basaltic volcanism in Mare Nubium. Such remote sensing data reveals subtle color differences of the basaltic units within the Mare [3]–[5], as well as compositional differences [6]–[9]. By processed Clementine data, Rose and Spudis indicated that Mare Nubium has undergone a prolonged and complex volcanic evolution [10]. Multiple flows of different age and composition have resurfaced the basin floor, and although the flows in Nubium are prominent, they are thin. Hiesinger studied ages and stratigraphy of the mare basalts and proposed that the lava flow units in Mare Nubium have a range of ages from Imbrian to Eratosthenian period (2.8–3.8 Ga), with most units having formed in the Late Imbrian period at 3.3–3.5 Ga [2]. Bugiolacchi *et al.* mapped the stratigraphy of Mare Nubium, and nine potential mare units are mapped and classified [see Fig. 1(b)], each with its characteristic chemical composition (FeO and TiO_2 abundances) and age [11]. Using LROC WAC data, Korokhin *et al.* consider this area as shallow flooding of an elevated formation of highland composition, the material of which could have been excavated and mixed up with upper layers of the lunar surface through meteoroid impacts [12]. A new geologic map around Mare Nubium has been drawn using CE-1 images, CE-2 images, imaging interferometer spectral data, and X-ray and Gamma-ray Spectroscopy data of CE-1 [13].

However, the penetration of the visible light and infrared radiation is only a few microns over the lunar regolith [11],

[1] https://planetarynames.wr.usgs.gov/Feature/3684

[14]. In this penetration depth, the lunar regolith is easily contaminated by the impact ejecta from the faraway distances [15]. Particularly, Ptolemaeus (1.8°W, 9.2°S, 153.7 km), Alphonsus (2.8°W, 13.4°S, 110.5 km), and Arzachel (1.9°W, 18.3°S, 97.0 km) craters locate near the eastern border of Mare Nubium. In addition, the ejecta from Bullialdus crater (22.2°W, 20.7°S, 60.7 km) within the Mare and Tycho crater (11.4°W, 43.3°S, 85.3 km) in the south clearly alter the regolith in the shallow layer, which makes it difficult to study the basaltic volcanism of Mare Nubium. To weaken the influence of the ejecta coverage, the earth-based radar data are employed, which indicate a new understanding of the lava flow complexes and reveal possible pyroclastic deposits hidden by the materials ejected from the highlands [16].

In China's CE-1 and 2 missions, the CELMS instrument has worked for more than 2 years. The penetration depth of the used microwave signal at 3.0 GHz can be up to several meters in the lunar regolith [14]. The microwave data are also sensitive to the substrate temperature and compositions of the lunar regolith and are less influenced by the surface topography [17]–[19]. These characteristics provide a new way to evaluate the basaltic units and volcanism in Mare Nubium.

In this article, the CELMS data from CE-2 satellite are used to evaluate the basaltic units in Mare Nubium. The rest of this article is organized as follows. In Section II, the brightness temperature (TB) of the basaltic unit is numerically studied with the radiative transfer simulation. The CELMS data processing is presented in Section III. Section IV briefly presents the TB features of basaltic units at daytime and night, as well as the corresponding TB difference features. Section V gives several important findings of the basaltic units in Mare Nubium, and the conclusions are given in Section VI.

II. TB of Basaltic Units

The interpretation and implication of the microwave data are the fundamental work needed to study the geology of the Nubium Basin. Therefore, to better understand the basaltic units with the TB and the TB difference (dTB) derived from the CE-2 CELMS data, the radiative transfer theory is used to theoretically study the thermophysical features of the regolith in the corresponding units.

The commonly used regolith model includes two layers, which are the regolith layer in the upper and the rock layer in depth. Considering that the observation angle of the CELMS instrument is 0°, the TB (or T_B) of the lunar regolith can be expressed as follows (suppose downward is the positive direction) [17], [19]:

$$\begin{aligned}\mathrm{TB} = &\int_0^{\mathrm{d}} \frac{1-r_1}{1-L} k_{a1}(z) T(z) \mathrm{e}^{-\int_0^z k_{a1}(z')\mathrm{d}z'} \mathrm{d}z \\ &+ \int_0^{\mathrm{d}} \frac{(1-r_1)r_2}{1-L} k_{a1}(z) T(z) \mathrm{e}^{-\left(\int_z^{\mathrm{d}} k_{a1}(z')\mathrm{d}z' + \int_0^{\mathrm{d}} k_{a1}(z')\mathrm{d}z'\right)} \mathrm{d}z \\ &+ \int_{\mathrm{d}}^{\infty} \frac{(1-r_1)(1-r_2)}{1-L} k_{a2}(z) T(z) \mathrm{e}^{-\int_{\mathrm{d}}^z k_{a2}(z')\mathrm{d}z'} \mathrm{d}z \\ &\cdot \mathrm{e}^{-\int_0^{\mathrm{d}} k_{a1}(z')\mathrm{d}z'} \end{aligned} \tag{1}$$

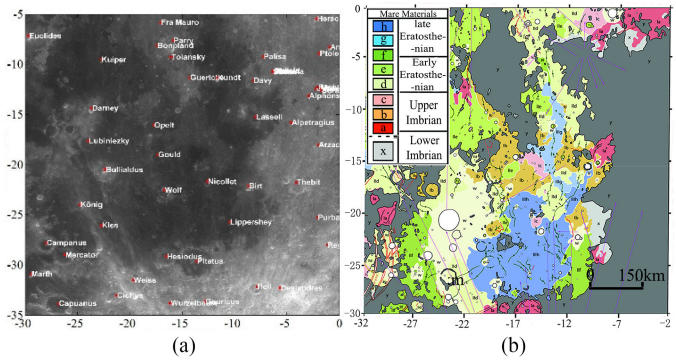

Fig. 1. (a) Geographical map and (b) geologic map [11] of Mare Nubium.

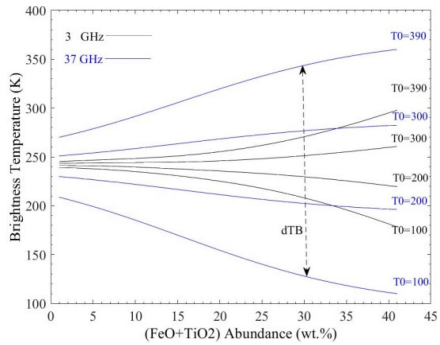

Fig. 2. Change of simulated TB with FTA and surface temperature [19].

where d is the regolith layer thickness; k_{a1} and k_{a2} are the absorption coefficients in the lunar regolith and rock layers, respectively; $T(z)$ is the temperature profile; r_1 and r_2 represent the effective reflectivity values of the free space–regolith and regolith–rock interfaces, respectively; and $1/(1-L)$ is the multireflection coefficient.

The decisive factor for the parameters of r_1, r_2, k_{a1}, and k_{a2} is the dielectric constant, which is expressed in the following [20]:

$$\begin{cases} \varepsilon' = 1.919^{\rho} \\ \tan\delta = 10^{0.038S + 0.312\rho - 3.260} \end{cases} \tag{2}$$

where ρ is the density of the lunar regolith; ε' is the real part of the dielectric constant, $\tan\delta$ is the loss tangent, and S (wt.%) is the ($\mathrm{FeO} + \mathrm{TiO_2}$) abundance (FTA).

Based on this, the relationship between the TB and the thermophysical parameters of the lunar regolith can be constructed. Here, d is assumed to be 5.7 m. The temperature profile is calculated with the thermal conductivity model and the outmost depth temperature is given as 252 K [21]. The hyperbolic model is used for ρ. The dielectric constant of the rock layer is assumed to be 6.15 + i0.155 (sample No.1555 from Apollo 15 mission). Thus, the change of TB with FTA in different surface temperature conditions can be simulated with (1), as well as dTB performances (see Fig. 2).

Fig. 2 indicates several important issues that are helpful to understand the microwave thermal emission features of the basaltic units.

First, considering that the younger basalts have higher FTA [10], [11], the TB of the younger basalts should be higher at daytime but lower at night compared to the basalts with lower FTA according to Fig. 2. This finding provides a chance to evaluate the basaltic units erupted at different times, including the testing of pyroclastic deposits with special thermophysical parameters.

Second, the dTB, defined as the difference of the same-channel TB from daytime to night, has been proved to be directly related to the regolith thermophysical features within the corresponding microwave penetration depth [18], [19], [22]. Fig. 2 indicates that the dTB is up to about 320 K at 37 GHz and about 100 K at 3.0 GHz (40 wt.% FTA), which is considerably higher than the TB changes: about 90 K (37 GHz) and 30 K (3.0 GHz) at noon and about 80 K (37 GHz) and 27 K (3.0 GHz) at night. Thus, a dTB map may propose a potentially important new way to study the basaltic units in Mare Nubium.

Third, the TB in different channels is the integration of the regolith parameters in the corresponding penetration depth, which means that the TB reflects the volumetric features of the basaltic units. This is useful to identify the mare basalts rearranged and masked by the ejecta of the craters in far distances.

Finally, the regolith thickness, surface slope, and roughness also play an essential role on the propagation of the microwave. However, the average regolith thickness is about 5.7 m in Mare Nubium [23], which is much thicker than the penetration depth of the microwave used by the CELMS instrument [19], [24]. Thus, the influence of the regolith thickness on the TB is neglected in this study. Furthermore, considering the observation angle of the CELMS instrument is 0°, the impact of the surface roughness can also be ignored. For the surface slope may alter the effective solar illumination, the evaluation of the TB and dTB performances should take the surface slope into account.

III. Data Processing

A. CELMS Data

The CELMS data used in this study were collected by the microwave sounder onboard the CE-2 satellite, which operated at 3.0, 7.8, 19.35, and 37.0 GHz from October of 2010 to May of 2011. The observation angle was 0°, and the temperature resolution was about 0.5 K. The original data we obtained were at the 2C-level after the system calibration and geometric correction, in Planetary Data System archive format. As a single file, the 2C-level data contain a header and a table of measured data, which includes the observation time, four-channel TB, solar incidence and azimuth angles, selenographic latitude and longitude, orbit altitude, and data quality state.

1) TB Maps Generation: The study area ranges from about 10°S to 30°S, 5°W to 30°W. First, the hour angle method is introduced to ascribe the selected TB points into 24 h combined with the solar incidence and azimuth angles and the selenographic latitude and longitude values read from header files [14], [17]. The purpose of this process is to weaken the TB variations brought by the observation time, since the surface temperature changes greatly with the observation time [20], [25], [26]. Then, the scatter maps are plotted to identify the proper hour angle, for the quantity of the CELMS data is not enough to cover the whole ranges of Mare Nubium in the 24-h angles. Through the comparisons of the scatter maps, the CELMS scatter plots from1 to 2 A.M. and from 9 to 10 A.M. are the relatively better candidates to represent the TB at daytime and nighttime. Finally, a seventh-degree polynomial fitting scheme was used to generate the TB maps at 3.0, 7.8, 19.35, and 37.0 GHz with a spatial resolution of 0.25° × 0.25° (see Fig. 3).

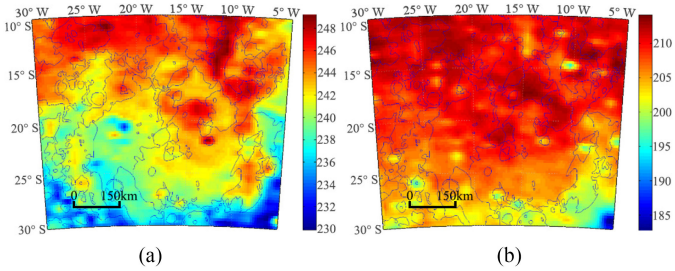

Fig. 3. TB maps of Mare Nubium at 37 GHz (unit: K). (a) Daytime. (b) Night (Lambert Conformal Conic projection).

In order to better understand the TB performances, the boundary of the basaltic units by Bugiolacchi *et al.* [11] is vectorized and overlaid on the TB and the following normalized TB (nTB) and dTB maps. Fig. 3 indicates a good correlation between the TB performances and the basaltic units, especially in Nicollet crater (12.5°W, 21.9°S) and its north section. Moreover, the visible ejecta rays in the spectral data [see Fig. 1(a)] are absent in the TB maps, indicating the relatively weaker influence of the impact ejecta on the TB of the original deposits of the basaltic units. Additionally, the basaltic units present different TB performances from daytime to nighttime. Thus, the TB maps provide a new understanding of the basaltic units in Mare Nubium compared to the optical data and even the radar observations.

Furthermore, Fig. 3 also shows that the variation of the TB with latitude is up to 20 K at daytime and night, which is much larger than that brought by the compositions of the lunar regolith in different basaltic units—no more than 5 K in the regions along the same latitude. Thus, the change of the TB with latitude must be weakened. In the previous studies, the nTB and dTB maps were proposed to weaken this effect [18], [19], [22], [27], which are also tried in this study.

2) nTB Maps Generation: To obtain the nTB maps, the standard TB values of every latitudes are proposed [18], [19], [22], [27]. At first, one TB is selected for every latitude on the conditions that the FTA, surface slope, and rock abundance are similar in all selected positions (the dots in Fig. 4), which can be read from the JMARS software. Second, a fitting curve is made according to the selected TB points (the solid line in Fig. 4), and the fitted value is defined as the standard TB for the corresponding latitude. Fig. 4 indicates that the fitting curves efficiently eliminate the random fluctuation of the selected TB in the places without identical regolith parameters, which represents standard TB at the given latitude. Finally, the nTB maps can be generated using the TB divided by the standard TB along the same latitude [18].

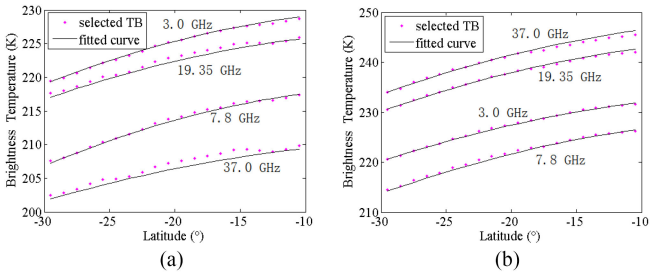

Fig. 4. Generation of standard TB. (a) Daytime. (b) Night.

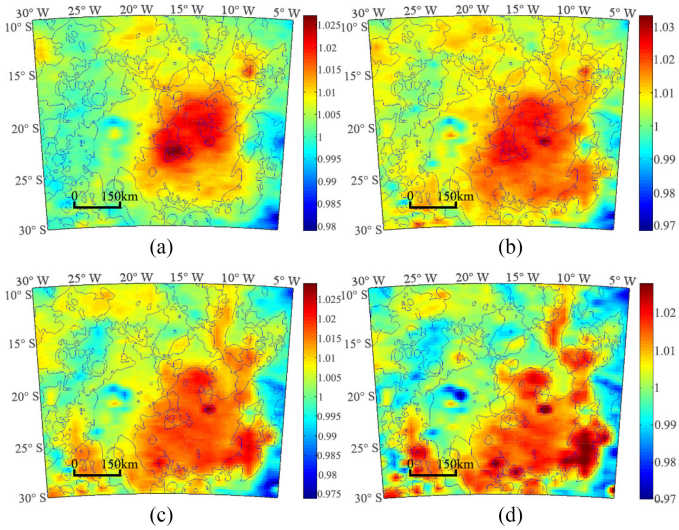

Fig. 5. nTB map of Mare Nubium at daytime. (Lambert Conformal Conic projection). (a) 3.0 GHz. (b) 7.8 GHz. (c) 19.35 GHz. (d) 37.0 GHz.

Through this method, the nTB maps at daytime (see Fig. 5) and night (see Fig. 6) are generated. Compared to Fig. 3, the change of the TB with the latitude is significantly weakened, which is clearly expressed in the nTB values along the 25°W longitude. However, the relatively higher nTB in the southern inner wall and the lower nTB in the northern inner wall of Bullialdus crater postulate that the surface slope still plays an important role in the generated nTB maps. Additionally, compared to the optical results [2], [11]–[13], the nTB maps at different channels and times show distinctly different views of the mare deposits in Mare Nubium, which will be discussed in the following section.

3) dTB Maps Generation: The dTB is defined as the difference between the daytime TB and the night TB of the same frequency, which is proposed to be directly related to the regolith thermophysical parameters within the penetration depth of the corresponding microwave [18], [19], [27]. Therefore, the dTB maps were also generated in this study (see Fig. 7). Interestingly, Fig. 7 indicates a largely good agreement between the geologic boundaries and the dTB performances, especially in unit IIf in the southern part of the Mare Nubium and units Ib and IId south to Fra Mauro peninsula. Moreover, the dTBs in the units with higher FTA are obviously higher than those with lower FTA, which corresponds with the simulation in Section II. In addition, the craters Guericke Kundt (11.6°W, 11.6°S), Birt

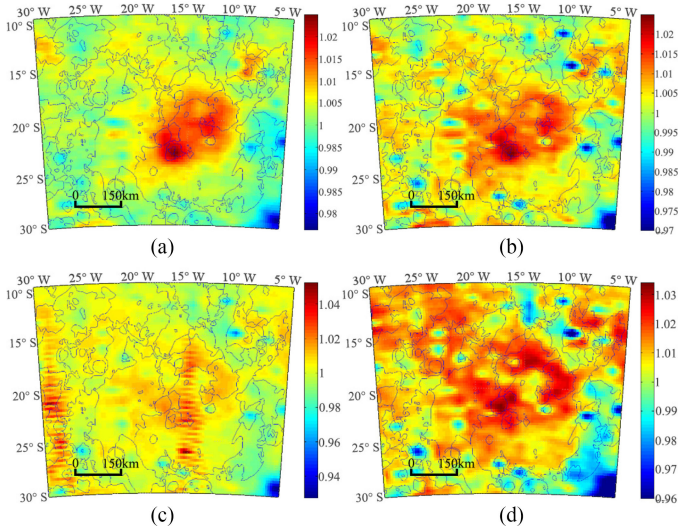

Fig. 6. nTB map of Mare Nubium at night (Lambert Conformal Conic projection). (a) 3.0 GHz. (b) 7.8 GHz. (c) 19.35 GHz. (d) 37.0 GHz.

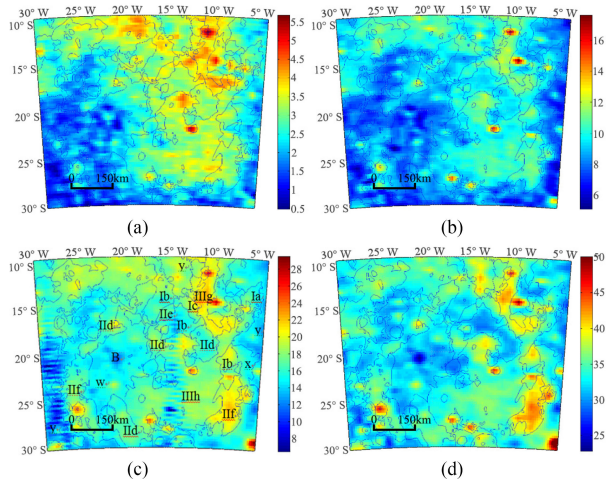

Fig. 7. dTB map of Mare Nubium (unit: K) (Lambert Conformal Conic projection). (a) 3.0 GHz. (b) 7.8 GHz. (c) 19.35 GHz. (d) 37.0 GHz.

(8.6°W, 22.4°S), Nicollet (12.5°W, 21.9°S) craters and several craters near Lassell (7.9°W, 15.5°S), Pitatus (13.5°W, 29.8°S) with larger dTB values and Bullialdus crater with lower nTB are clearly presented in Fig. 5. This outcome proves that the generated TB maps are rational in the values and the positions.

Furthermore, Figs. 3 and 5 depict that the nTB in the southern inner wall is higher than that in the northern part of Bullialdus crater, whereas Fig. 7 shows an evenly distributed low dTB similar to the FTA in the following Fig. 8, as well as to the other craters. This means that the surface slope plays a minor role on the generated dTB maps. Thus, the dTB will provide a specially important role in understanding the basaltic units in Mare Nubium.

B. Clementine UV/VIS Data

FeO and TiO_2 abundances are the important parameters to change the absorption feature of the lunar regolith [14]. The

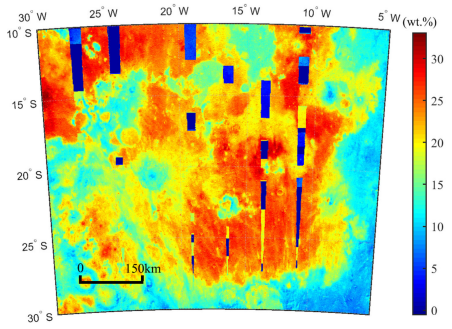

Fig. 8. FTA map of Mare Nubium (Lambert Conformal Conic projection).

TABLE I
AVERAGE DTB AND FTA OF THE IMPORTANT UNITS

Unit	Log	Lat	dTB (K) / Channel (GHz)				FTA wt.%
			3.0	7.8	19.35	37.0	
Ia	-6.4°	-14.0°	2.9	9.1	16.1	33.2	18.0
Ib	-14.3°	-17.0°	3.3	9.7	15.5	31.4	21.3
Ib	-8.6°	-20.6°	3.0	10.1	18.6	37.4	19.0
Ib	-16.7°	-13.7°	3.4	9.7	17.2	33.7	20.3
Ic	-13.4°	-15.3°	3.8	10.6	18.1	35.1	21.6
IId	-11.5°	-19.0°	3.3	9.6	16.4	31.8	22.0
IId	-17.1°	-18.8°	3.2	9.9	17.6	34.2	23.7
IId	-20.4°	-27.7°	2.1	8.6	16.6	34.6	17.4
IId	-22.3°	-17.0°	2.7	9.3	16.7	33.5	22.0
IIe	-15.8°	-15.9°	3.5	10.0	16.7	32.9	23.7
IIf	-8.6°	-25.7°	3.0	10.4	20.0	40.0	18.6
IIf	-25.7°	-24.6°	1.9	8.7	16.6	34.5	19.4
IIIg	-11.2°	-14.3°	3.9	11.3	20.6	38.8	25.5
IIIh	-14.2°	-23.7°	3.1	10.0	17.3	35.1	24.0
w	-21.5°	-21.8°	2.1	8.1	15.3	31.9	19.1
x	-6.5°	-21.6°	2.3	8.3	15.8	34.4	12.0
y	-6.4°	-15.2°	2.5	8.2	14.8	32.2	12.3

methods developed by Lucey *et al.* [7] are widely used to retrieve the FeO and TiO_2 abundances with Clementine ultraviolet/visible (UV/VIS) data, which are also employed in this study to obtain the FTA map of Mare Nubium (see Fig. 8). Here, the FTA result is validated with that obtained by Bugiolacchi *et al.* [11] and by Wu [28] with the CE-1 IIM data.

Fig. 8 shows that the relatively higher FTA occurs in the central, southern, and eastern parts of Mare Nubium, whereas the FTA in the western part is relatively lower. The regions within Bullialdus crater and surrounding Wolf crater (16.6°W, 22.8°S) postulate the lowest FTA.

IV. RESULTS

Figs. 5–7 present a different view of Mare Nubium compared to the optical and radar results.

A. nTB Features of Basaltic Units

According to the compositions and estimated age of the lunar regolith, the lava basalts in Mare Nubium are separated into the Late Imbrian Epoch (I), the early Eratosthenian Period (II), and the late Eratosthenian Period (III) as shown in Figs. 1(b) and 7(c) [11]. Figs. 3, 5, and 6 indicate a fairly weak correlation between the nTB performances and the basaltic units.

At daytime, the nTB performances largely agree with the FTA distributions, where the higher FTA in the eastern part of Mare Nubium corresponds well with the larger nTB here, and vice versa for the western part. However, the detailed nTB performances are hard to understand by the optical results. At 3.0 GHz, the nTB is highest in the central Nubium, and the ranges include the northern part of unit IIIh and the nearby units Ib and IIe in the west and units IId and Ic in the east. At 7.8 GHz and 19.35 GHz maps, the regions with the highest nTB extend in the south and east directions, and the relatively higher nTB also occurs in the southwestern part of Mare Nubium, just west to the Kies (22.6°W, 26.3°S) and Konig (24.7°W, 24.2°S) craters. Only at 37 GHz map do the dTB performances show a positive correlation with the basaltic units identified by Bugiolacchi *et al.* [11], but the highest nTB occurs in units IIf and Ia in the southeastern part of Mare Nubium.

At night, the nTB indicates a rather complex understanding of the basaltic units. As mentioned in Section II, the regions with higher FTA should have lower TB and nTB at night, which is verified by the nTB performances in Nicollet crater, unit IIIg east to Fra Mauro peninsula, and units IIf and Ia in the southeastern part of Mare Nubium. However, the nTB performances at 3.0 and 7.8 GHz are still highest in the central Nubium, and the range is slightly smaller than that at daytime. This phenomenon is even worse at 37 GHz, where the differences between the eastern and western Mare Nubium are hard to recognize.

Additionally, several special nTB performances should be mentioned.

First, in unit Ib centered at (10°W, 14°S), both the 3.0 GHz dTB values at daytime and night are similarly high as the central Nubium, while the ranges of the daytime and night nTB are much smaller than those of the latter.

Second, the patch near Wolf crater (17.6°W, 16.3°S) has the highest 3.0 GHz nTB at daytime, while it is similar to its vicinity at the 7.8 and 19.35 GHz maps, but it is lower than its vicinity at 37 GHz. At night, this patch presents the highest nTB at 3.0 and 7.8 GHz maps, while it is similar to its vicinity at 37 GHz. Combined with the penetration depth of the used microwave [19], [24], this means that the thermophysical parameters of the mare deposits are changing greatly with depth in this place.

Moreover, one thing that puzzled us is that the FTA here is rather low as shown in Fig. 8, which is therefore identified as highlands materials in Fig. 1(b). Such low FTA could not support the highest 3.0 GHz nTB both at daytime and night according to the theoretical simulation in Section II.

Third, to unit IIf in the western part of Mare Nubium, the nTB is similar to the nearby regions at 3.0 GHz both at daytime and at night, but it is apparently higher at daytime and lower at night than the nearby regions at the other three channels. This nTB performance agrees with the simulation results in Section II. Moreover, this also indicates a rather thin layer of mare deposits in the region if the penetration features of the used microwave are considered.

Fourth, unit w surrounding Bullialdus crater has the lowest nTB at daytime but the relatively higher nTB at night, which is rational according to the theoretical simulation in Section II because of the lower FTA occurring in this region.

Unit x centered at (6°W, 20°S) is considered to be remnants of the oldest exposed basaltic flows, which shows compositions similar to the neighboring highlands [11]. The nTB in this unit is lower than the neighboring highlands both at noon and at night, indicating the particularity of the regolith deposits in this region.

Finally, there occur abundant craters with rather low nTB at nighttime 7.8 and 37 GHz maps, including Kundt, Birt, Nicollet craters, and several craters near Lassell, Pitatus (13.5°W, 29.9°S), Campanus (27.9°W, 28.0°S), Lubiniezky (23.9°W, 17.9°S), and Opelt (17.6°W, 16.3°S). However, they are not clear at 3.0 GHz and the four channels at daytime.

These phenomena will be further discussed in the following section.

B. dTB Features of Basaltic Units

The simulation results in Section II indicate that the highlands with the lowest FTA should have the lowest dTB values, which is verified by the dTB performances in the east and southwest parts of the study area. The dTB is the second-lowest in the western Nubium, and the highest dTB exists in the basaltic units in the eastern part of Mare Nubium, including units IIIg, Ib, and IIf. Moreover, for unit IIIh in central Nubium with the highest nTB at daytime and night, only the northern part of the unit indicates the highest- and second-highest dTB values. Generally, within Mare Nubium, the dTB performances can be categorized into the following three regions.

The first region includes unit IIf with green color in the southeastern and western parts in Fig. 1(b), where the FTA is lower than the central Nubium but higher than the nearby highlands. The dTB in the southeastern part is second highest, similar to the central Nubium at 3.0 and 7.8 GHz, but it is much higher than the central part at 19.35 and 37 GHz. In the western part, the dTB is similar to the nearby highlands at 3.0 GHz, but it is similar to the central Nubium at the other three channels. These both mean the change of regolith thermophysical parameters with depth. Also, the mare deposit in the western part is different from the southeastern part in the depth layer.

The second region is mainly unit IIIh with blue color in the central Nubium in Fig. 1(b), where the FTA is nearly highest in Mare Nubium. However, the dTB maps indicate that there exists a dTB anomaly in the northern part centered at (14.8°W, 19.3°S), where the dTB is clearly higher than the other places of the unit. Moreover, the dTB performances of unit IIIg in the northeastern part are similar to the high dTB anomaly, indicating the homogeneity of the regolith in depth revealed by the CELMS data. Unfortunately, this also means the different mare deposits of IIIh unit beyond the anomaly.

The third region is unit w in the middle-western part of Mare Nubium, where the FTA is a bit higher than the highlands but apparently lower than the second region above. However, the dTB is as low as the highlands at the four channels. Here, the Bullialdus crater indicates the relatively lower FTA and lowest dTB values. Considering the cratering mechanism brought by Bullialdus crater, the lowest dTB means the special materials existed in this region.

What astonished us are the dTB performances in units centered at (26°W, 26°S) and (17.7°W, 27.1°S). Here, they are categorized into unit w as that surrounding Bullialdus crater. However, their dTB values are much higher than those surrounding Bullialdus crater, which are similar to the dTB of unit IIIg in the northeastern part. This finding means that the mare deposits here are different from those surrounding Bullialdus crater, though they belong to the same geologic unit.

Moreover, the dTB performances in the four channels are also different.

At 3.0 GHz, the relatively lower dTB mainly occurs in the highlands and the western units including IIf and w and unit IId in the southern part. At the other three channels, the regions with relatively lower dTB extend to the east, which reaches units Ib and IId near the north part of unit IIIh. Meanwhile, unit IId in the southern part indicates a higher dTB similarly to unit IIIh. Considering the penetration ability of the microwave used by the CELMS instrument, this again means the change of the regolith thermophysical parameters with depth in these basaltic units.

Considering the dTB is obtained by subtracting the night TB from the daytime TB, the results are hoped to be less affected by the thermophysical parameters of the substrate deposits and be directly related to the regolith thermophysical parameters within the penetration depth of the used microwave. This will be a meaningful supplement to improve understanding the nTB performances of the basaltic units.

V. New View of Mare Nubium

The nTB and dTB performances indicate a complex understanding of Mare Nubium.

A. High nTB Anomaly

The high nTB anomaly will mislead us in understanding the thermophysical features of the basaltic units in the microwave range. Thus, it is discussed first.

In Section IV-A, we found that the nTB performances in the patch near Wolf crater are abnormal, for the low FTA here could not support the fairly high nTB both at daytime and night according to the theoretical simulation in Section II. The range of the anomaly can be extended to the whole central part of Mare Nubium, which makes it difficult to understand the basaltic units at 3.0, 7.8, 19.35 GHz maps at daytime and the nighttime maps.

A similar phenomenon also occurs in Maria Moscoviense and Orientale. After studying the regolith thermophysical parameters with the theoretical simulation, Meng *et al.* [19], [29] proposed that the higher substrate temperature should be responsible for the nTB anomaly of this kind.

Here, the dTB maps are proposed to eliminate the influence of the substrate temperatures [18], [19], [27]. Interestingly, Fig. 7 postulates a relatively lower dTB at 3.0 GHz in the patch near Wolf crater, which is similar to unit w surrounding Bullialdus crater. Moreover, the dTB at 3.0 GHz in central Nubium is similar to the most extensive regions in the middle and eastern parts

of Mare Nubium, indicating the homogeneity of the regolith thermophysical features in the shallow layer. Thus, there are no special materials supporting the high nTB anomaly at 3.0 GHz. This validates that only the higher substrate temperature can support the higher daytime and nighttime nTB.

Moreover, the daytime nTB of unit IIIg in the eastern part, unit IIf in the southeastern part, and the units IId and IIf in the southwestern part is clearly higher than the nighttime nTB, which agrees well with the relatively higher FTA according to the theoretical simulation in Section II. This again verifies that the higher substrate temperature is likely the cause for the high nTB anomaly of the central Nubium. If so, this will be the largest region with the high TB anomaly ever discovered over the lunar surface.

Elphic *et al.* [8] indicated that radioactive elements are abnormally high in Mare Nubium, which may support our hypothesis about the higher substrate to some extent. Moreover, Ji *et al.* [30] proposed an uplift using the LRO LOLA data, and the position of the uplift largely agrees with the hot anomaly. This implies that the possible relationship between the uplift and the nTB anomaly. Additionally, Korokhin *et al.* [12] found a photometric anomaly (17.7°W, 21.6°S), which is just inside the hot anomaly. The simultaneous existences of the high nTB anomaly, the high radioactive elements anomaly, the uplift, and the photometric anomaly all help to provide a new view on the thermal evolution of Mare Nubium.

The hot anomaly is centered at (15°W, 21.5°S). The shape of the anomaly is an ellipse with about 240 km in length and 180 km in width. This is the largest hot anomaly we met when studying the substrate thermal anomaly with the CELMS data. We have evaluated the hot anomaly in Mare Moscoviense [19], but its size is much less than this anomaly. Also, the hot anomaly does not affect our comparison between the CELMS data and optical results. The hot anomaly in central Nubium has heavily altered the thermal emission features of the basaltic units, indicating that the intensity is high.

In addition, the nTB performances in unit Ib centered at (10°W, 14°S) show that it is another region with the hot anomaly. The double existences of the hot anomalies and the high intensity again imply the particularity of Mare Nubium in studying the thermal evolution of the Moon, which deserves to be further studied with more sources of data.

This finding also gives a rational interpretation of the complex nTB performances in Mare Nubium as mentioned in Section IV.

B. Basaltic Units

To better understand the microwave thermophysical features of the deposits in Mare Nubium, the average dTB and FTA values of the important basaltic units are presented in Table I. The complex of the basaltic units is expressed as follows.

First, the nTB and dTB performances in the northeastern unit IIIg agree well with its younger age and highest average FTA. However, although unit IIIh in central Nubium is similar to unit IIIg in age and average FTA, the dTB in most places is much lower than that in unit IIIg. Even in unit IIIh, the dTB in the northern part is higher than the regions beyond the north, meaning the different mare deposits in the northern part. We mentioned that the unit is heavily contaminated by the impacted ejecta indicated by Figs. 1(a) and 8. Thus, the dTB performances show that the current geologic identification is not enough only using the optical data.

Second, the nTB performances postulate a negative view on the relationship between the FTA of the basaltic unit and its age. Bugiolacchi *et al.* [11] proposed that the FTA is largely increasing with the younger ages of the basaltic unit in Mare Nubium. Moreover, according to the simulation in Section II, the units with higher FTA should have higher nTB at daytime, lower nTB at night, and higher dTB values [19], [31]. Therefore, the units marked III in the late Eratosthenian Period should have the highest daytime nTB, the lowest night nTB, and the highest dTB. However, the nTB and dTB performances do not support the conclusion. The abnormal nTB performances can be attributed to the relatively higher substrate temperature. Nevertheless, the dTB performances hint the change of the regolith parameters with depth in the basaltic units.

This is particularly apparent in unit IIf in the southeastern part. Here, the average dTB at 3.0 GHz is 3.0 K, approximating the 3.1 K in the west unit IIIh. However, from 7.8 GHz, the dTB in unit IIf becomes apparently higher than unit IIIh, which is even higher than unit IIIg with the highest average FTA in the northeastern part. Considering the penetration features of the used microwave [19], [24], this means that the mare deposit in depth below 100 cm (3.0 GHz microwave penetration depth in the regolith with higher FTA) is low in FTA as the west unit IIIh. It is fairly rich in FTA from 38.5 cm (7.8 GHz microwave penetration depth) to 16.2 cm (37 GHz microwave penetration depth in the regolith with lower FTA). Interestingly, the average FTA estimated with Clementine UV/VIS data here is only 18.6 wt.%. This means that the regolith of the unit is heavily contaminated with the materials with lower FTA in the shallow layer. Moreover, the nTB performances also support the FTA-rich deposits in depth layer, as discussed in the previous section. This also means a rather thin layer of mare deposits here, less than 1 m.

Notably, the famous straight wall and Rima Birt also exist in this unit. Combined with the thin basalt layer, this hints that the basaltic volcanism in the southeastern unit IIf may be fairly significant in Mare Nubium.

Furthermore, this finding brings a new problem to understand the relationship between the FTA and the age of the basaltic units. Xiao *et al.* [32] and Meng *et al.* [18] both mentioned the accuracy of the age method by crater counting. The mare basalts with a thin layer and heavy surface contamination exacerbate the problem. Thus, how to identify the age of such units will be a new topic of the basaltic volcanism study.

Third, unit w is the impact ejecta mainly distributed surrounding Bullialdus crater, which has the lowest daytime nTB, the relatively higher night nTB, and the lowest dTB. However, the patches of unit w centered at (26°W, 26°S) and (17.7°W, 27.1°S) indicate a considerably high dTB, meaning that the deposit here is different from that surrounding Bullialdus crater.

Meanwhile, the units centered at (15.3°W, 27.9°S) and at Nicollet crater also show the similar nTB and dTB performances

as those centered at (26°W, 26°S) and (17.7°W, 27.1°S). These nTB and dTB performances indicate a fairly high FTA enriched in the mare deposits according to the simulation in Section II. Bugiolacchi *et al.* [11] suggested the local chemical anomalies occurring in the unit centered at (15.3°W, 27.9°S). Thus, more work should be done to explain the TB and composition anomaly of this kind.

Finally, the nTB and dTB performances in unit IId centered at (11.5°W, 19.0°S) are apparently different from those in unit IId centered at (20.4°W, 27.7°S), which indicates the similar surface features in optical data. Moreover, the nTB and dTB performances in unit IId centered at (11.5°W, 19.0°S) are similar as those in unit Ib centered at (14.3°W, 17.0°S), which indicates the different surface features in optical data.

A similar phenomenon also happens to abundant basaltic units, again showing the complexity of the mare deposits in Mare Nubium.

Even so, the dTB maps and the daytime nTB map at 37 GHz clearly indicate that the mare basalts in the units near the east margin of Mare Nubium is considerably young, followed by the mare basalts in the central Nubium, and those in the western Nubium are oldest. However, even in the units near the east margin, the dTB and nTB performances indicate that the mare basalts in the northern part are high in FTA, whereas unit IIf in the southern part only has a thin layer of FTA-rich basalt and its surface layer is covered by the deposits with a relatively lower FTA. The complex dTB and nTB performances of the mare deposits prohibit us to give a new interpretation of the basaltic volcanism in Mare Nubium with only the CELMS data.

C. Possible Pyroclastics

The floor of Lassell crater has been previously identified as having spectral characteristics indicative of pyroclastic deposits [33]. Carter *et al.* [16] suggested a larger area of pyroclastic deposits including Lassell crater and the highlands to the west using the earth-based radar data. The pyroclastic deposits have been proved to have the special dielectric features [16], [33], which should be detected by the CELMS instrument. However, no special nTB and dTB performances are found in the aforementioned places. Maybe this phenomenon can in part be attributed to the strong thermal anomaly in central Nubium

Therefore, Mare Nubium is not a proper place to study the thermophysical features of the pyroclastics with the CELMS data.

D. The Cold Anomaly

In Section IV, we mentioned several cold spots in the night nTB maps. The causes of these cold spots are not clear. At night, abundant craters show the very low nTB at 7.8 and 37 GHz maps, including Kundt, Birt, Nicollet craters, and several craters near Lassell, Pitatus, Campanus, Lubiniezky, and Opelt. These craters present very high dTB values. Chan *et al.* [34], Zheng *et al.* [14], Gong and Jin [35], and Meng *et al.* [18], [27] suggested that the TB in the craters with abundant rocks will be higher at noon and lower at night. Here, the night nTB and dTB performances at 7.8, 19.35, and 37 GHz agree with the previous studies. However, the anomaly in the aforementioned craters is not clear at 3.0 GHz, indicating that the deposits brought the cold anomaly occur in the shallow layer, less than 2 m penetrated by the 3.0 GHz microwave in such regions. Moreover, the anomaly is also not clear at daytime. This may be attributed to the observation time, from 9 to 10 o'clock, and the difference between the special deposits and the normal regolith is likely not enhanced at this time. Thus, what is the best time to measure the mare deposits and the rock information should be taken into consideration in future.

Moreover, the low dTB anomaly also occurs in the western part of Mare Nubium, mainly including unit w, defined as ejecta blankets by Bugiolacchi *et al.* [11]. It is recognized as the basaltic units covered by the impact ejecta [11]. However, the basaltic deposits are not revealed by the CELMS data. Thus, if they are the impact ejecta, their source is in doubt for the following two reasons. First, Bullialdus crater is not responsible to the source, since Fig. 8 indicates that most ejecta are in the northwest direction but not centered at the crater [11]. Second, they are also not attributed to Tycho crater, for the ejecta thickness should be rather thin according to the cratering mechanism [35]. Then, the low dTB anomaly should not be attributed to the impact ejecta. If so, the deposits here should be the regolith mainly located in the original places. That is, the unit with low dTB and low TA is the Mare floor deposits produced during the formation of Mare Nubium.

To verify our deduction, the 70-cm earth-based radar results by Carter *et al.* [16] are also introduced. The radar map presented by Carter *et al.* [16] only reaches the near-western part of Bullialdus crater. Even so, the radar tone in the low dTB anomaly is different from that in the central Nubium, also indicating the difference between the two regions in the compositions of the deposits. Moreover, the radar tone in the low dTB anomaly is similar to that of Bullialdus crater. Combined with the penetration abilities of the microwave used by the CELMS instrument and the earth-based radar, this verifies that the deposits in the low dTB anomaly are homogeneous from the shallow layer penetrated by the 37-GHz microwave to the depth represented by the 70-cm radar microwave.

Therefore, the unit with low dTB and FTA in the western Nubium is likely the Mare floor deposits produced during the formation of Mare Nubium.

VI. Conclusion

In this article, combined with the FTA derived from Clementine UV/VIS data and the geologic identification by Bugiolacchi *et al.* [11], the CE-2 CELMS data were used to study the microwave thermophysical features of the basaltic units in Mare Nubium. The main results are as follows.

1) Two regions with hot anomaly are found in Mare Nubium. The hot anomaly in the central Nubium is extensive in range and high in intensity. Their causes are suggested to be the high substrate temperature.
2) The nTB performances postulate a negative view of the relationship between the FTA of the basaltic unit and its age. The nTB and dTB performances verify the contamination of the impact ejecta in the superficial layer. Also, a very

thin layer of mare basalt is revealed in the southeastern part of Mare Nubium.

3) The nTB and dTB maps postulate the different performances for the basaltic units in same epochs and the similar performances for the basaltic units in different epochs, indicating the complexity of the mare deposits in Mare Nubium.
4) Combined with the 70-cm earth-based radar results, the cold dTB anomaly in the western part of Mare Nubium is proposed as the Mare floor deposits produced during the formation of Nubium basin.

Additionally, the simultaneous occurrences of the high nTB anomaly, the uplift, the radioactive elements, and photometric anomalies in the regions near Wolf crater suggest a new view about the thermal evolution of Mare Nubium, which deserves to be further studied with more sources of data.

ACKNOWLEDGMENT

The authors would like to express their thanks to the people helping with this work. In this study, the WAC data were downloaded from http://wms.lroc.asu.edu/lroc/search, and the UV/VIS data were downloaded from http://webgis.wr.usgs.gov/pigwad/down/moon_dl.htm.

REFERENCES

[1] D. E. Wilhelms, in *The Geologic History of the Moon (U.S. Geological Survey Professional Paper)*. Washington, DC, USA: US Government Publishing Office, 1987.
[2] H. Hiesinger, "Ages and stratigraphy of mare basalts in Oceanus Procellarum, Mare Nubium, Mare Cognitum, and Mare Insularum," *J. Geophys. Res.*, vol. 108, 2003, Art. no. 5065.
[3] S. G. Jin, S. Arivazhagan, and H. Araki, "New results and questions of lunar exploration from SELENE, Chang'E-1, Chandrayaan-1 and LRO/LCROSS," *Adv. Space Res.*, vol. 52, no. 2, pp. 285–305, 2013.
[4] T. B. McCord, C. M. Pieters, and M. A. Feierberg, "Multi-spectral mapping of the lunar surface using groundbased telescopes," *Icarus*, vol. 29, no. 1, pp. 1–34, 1976.
[5] C. M. Pieters, "Mare basalt types on the front side of the Moon," in *Proc. Lunar Planet Sci. Conf.*, 1978, vol. 3, no. 9, pp. 2825–2849.
[6] D. J. Lawrence *et al.*, "Thorium abundances on the lunar surface," *J. Geophys. Res.*, vol. 105, pp. 20307–20331, 2000.
[7] P. G. Lucey, D. T. Blewett, and B. L. Jolliff, "Lunar iron and titanium abundance algorithms based on final processing of Clementine ultraviolet/visible images," *J. Geophys. Res. Planets*, vol. 105, no. E8, pp. 20297–20305, 2000.
[8] R. C. Elphic *et al.*, "Lunar rare earth element distribution and ramifications for FeO and TiO_2: Lunar prospector neutron spectrometer observations," *J. Geophys. Res.*, vol. 105, pp. 20333–20345, 2000.
[9] R. C. Elphic *et al.*, "Lunar prospector neutron spectrometer constraints on TiO_2," *J. Geophys. Res.*, vol. 107, 2002, Art. no. 5024.
[10] D. E. Rose and P. D. Spudis, "Piercing the clouds: The stratigraphy of Mare Nubium," in *Proc. Lunar Planet. Sci. Conf.*, 2000, Art. no. 1364.
[11] R. Bugiolacchi *et al.*, "Stratigraphy and composition of lava flows in Mare Nubium and Mare Cognitum," *Meteoritics Planet Sci.*, vol. 41, no. 2, pp. 285–304, 2006.
[12] V. Korokhin *et al.*, "Characterization of a photometric anomaly in lunar Mare Nubium," *Planet. Space Sci.*, vol. 122, pp. 70–87, 2016.
[13] J. Z. Liu *et al.*, "New geologic map of the LQ-19 (Mare Nubium) quadrangle on the Moon," in *Proc. 48th Lunar Planet. Sci. Conf.*, 2017, Art. no. 1447.
[14] Y. C. Zheng *et al.*, "First microwave map of the Moon with Chang'E-1 data: The role of local time in global imaging," *Icarus*, vol. 219, no. 1, pp. 194–210, 2012.
[15] J. F. Mustard and J. W. Head, "Buried stratigraphic relationships along the southwestern shores of Oceanus Procellarum: Implications for early lunar volcanism," *J. Geophys. Res.*, vol. 101, pp. 18913–18926, 1996.
[16] L. M. Carter *et al.*, "Earth-based radar and orbital remote sensing observations of mare basalt flows and pyroclastic deposits in Mare Nubium," in *Proc. Lunar Planet. Sci. Conf.*, 2017, p. 1736.
[17] S. J. Keihm and M. G. Langseth, "Microwave emission spectrum of the Moon: Mean global heat flow and average depth of the regolith," *Science*, vol. 187, pp. 64–66, 1975.
[18] Z. G. Meng *et al.*, "MTE features of Apollo Basin and its significance in understanding the SPA Basin," *IEEE J. Sel. Topics Appl. Earth Observ. Remote Sens.*, vol. 12, no. 7, pp. 2575–2583, Jul. 2019.
[19] Z. G. Meng *et al.*, "Reevaluating Mare Moscoviense and its vicinity using Chang'E-2 microwave sounder data," *Remote Sens*., vol. 12, no. 3, 2020, Art. no. 535.
[20] G. H. Heiken, in *Lunar Sourcebook: A User's Guide to the Moon*. London, U.K.: Cambridge Univ. Press, 1991.
[21] S. J. Keihm, "Effects of subsurface volume scattering on the lunar microwave brightness temperature spectrum," *Icarus*, vol. 52, pp. 570–584, 1982.
[22] Z. G. Meng et al.*et al.*, "Passive microwave probing mare basalts in Mare Imbrium using CE-2 CELMS data," *IEEE J. Sel. Topics Appl. Earth Observ. Remote Sens.*, vol. 11, no. 9, pp. 3097–3104, Sep. 2018.
[23] Y. G. Shkurato and N. V. Bondarenko, "Regolith layer thickness mapping of the Moon by radar and optical data," *Icarus*, vol. 149, pp. 329–338, 2001.
[24] B. A. Campbell *et al.*, "Volcanic and impact deposits of the Moon's Aristarchus Plateau: A new view from earth-based radar images," *Geology*, vol. 36, pp. 135–138, 2008.
[25] Z. G. Meng *et al.*, "Influence of lunar topography on simulated surface temperature," *Adv. Space Res.*, vol. 54, pp. 2131–2139, 2014.
[26] Y. C. Zhu *et al.*, "Analysis of the brightness temperature features of the lunar surface using 37 GHz channel data from the Chang'E-2 microwave radiometer," *Adv. Space Res.*, vol. 63, no. 1, pp. 750–765, 2019.
[27] Z. G. Meng, Q. Wang, H. Wang, T. Wang, and Z. Cai, "Potential geologic significances of Hertzsprung basin revealed by CE-2 CELMS data," *IEEE J. Sel. Topics Appl. Earth Observ. Remote Sens.*, vol. 11, no. 10, pp. 3713–3720, Oct. 2018.
[28] Y. Z. Wu *et al.*, "Global estimates of lunar iron and titanium contents from the Chang'E-1 IIM data," *J. Geophys. Res. Planets*, vol. 117, no. E2, pp. 1–23, 2012.
[29] Z. G. Meng, J. Zhang, Z. Cai, J. Ping, and Z.-S. Tang, "Microwave thermal emission features of Mare Orientale revealed by CELMS data," *IEEE J. Sel. Topics Appl. Earth Observ. Remote Sens.*, vol. 10, no. 6, pp. 2991–2998, Jun. 2017.
[30] J. Z. Ji *et al.*, "Impact basin of Mare Nubium: Reconstruction and geological evolution," *Acta Petrologica Sin.*, vol. 32, no. 1, pp. 127–134, 2015.
[31] Z. Z. Wang *et al.*, "Lunar surface dielectric constant, regolith thickness, and 3He abundance distributions retrieved from the microwave brightness temperatures of CE-1 Lunar Microwave Sounder," *Sci. China Earth Sci.*, vol. 53, no. 9, pp. 1365–1378, 2010.
[32] L. Xiao *et al.*, "A young multilayered terrane of the northern Mare Imbrium revealed by Chang'E-3 mission," *Science*, vol. 347, no. 6227, pp. 1226–1229, 2015.
[33] L. R. Gaddis *et al.*, "Compositional analyses of lunar pyroclastic deposits," *Icarus*, vol. 161, pp. 262–280, 2003.
[34] K. L. Chan *et al.*, "Lunar regolith thermal behavior revealed by Chang'E-1 microwave brightness temperature data," *Earth Planet. Sci. Lett.*, vol. 295, no. 1–2, pp. 287–291, 2010.
[35] X. H. Gong and Y. Q. Jin, "Diurnal change of thermal emission with "hot spots" and "cold spots" of fresh lunar craters observed by Chinese Chang'E-1," *Sci. China-Inf. Sci.*, vol. 42, no. 8, pp. 923–935, 2012.
[36] Z. Y. Yue *et al.*, "Projectile remnants in central peaks of lunar impact craters," *Nature Geosci.*, vol. 6, no. 6, pp. 435–437, 2013.

Zhiguo Meng (Member, IEEE) received the Ph.D. degree in geophysics from Jilin University, Changchun, China, in 2008.

He is currently a Professor with the College of Geoexploration Science and Technology, Jilin University. He has authored and co-authored more than 70 scientific papers. His research interests include the application and development of microwave remote sensing technology in the planetary science, primarily the microwave measurement of the lunar regolith.

Shengbo Chen (Member, IEEE) received the Ph.D. degree in earth exploration and information technology from Jilin University, Changchun, China, in 2000.

He is currently a Professor with the College of Geoexploration Science and Technology, Jilin University. He is also a Researcher with the CAS Center for Excellence in Comparative Planetology, Hefei, China. He has authored and coauthored more than 200 scientific papers. His research interests include information mechanism of remote sensing, inversion of land surface physical parameters, lunar and planetary remote sensing, the processing methods of remote sensing data, inversion of earth and lunar surface rock mineral composition based on hyperspectral remote sensing, and the research on technology and method based on comprehensive application of remote sensing, Beidou, and communication satellites.

Yongzhi Wang received the Ph.D. degree in geoexploration and information technology from Jilin University, Changchun, China, in 2008.

He is currently a Professor with the College of Geoexploration Science and Technology, Jilin University. From 2015 to 2016, he was a Visiting Scholar with York University, Toronto, ON, Canada. He has authored and co-authored more than 50 scientific papers. His research interests include remote sensing, geoscience big data, and artificial intelligence.

Prof. Wang is a Member of the International Association for Mathematical Geosciences.

Weiming Cheng received the Ph.D. degree in cartography and geographical information system from the State Key Laboratory of Resources and Environmental Information System, Institute of Geographic Sciences and Natural Resources Research, Chinese Academy of Science, Beijing, China, in 2003.

He is currently a Professor with the Institute of Geographic Sciences and Natural Resources Research, Chinese Academy of Sciences. His research interests include digital geomorphologic analysis, information extraction, digital geomorphologic mapping, and geomorphologic basic application research of ecoenvironmental change.

Shuanggen Jin (Member, IEEE) received the Ph.D. degree in geodesy from the University of Chinese Academy of Sciences, Beijing, China, in 2003.

He is currently a Professor and the Dean of the Nanjing University of Information Science and Technology, Nanjing, China, and also a Professor with Shanghai Astronomical Observatory, CAS, Shanghai, China. He has authored and co-authored more than 400 papers in international peer-reviewed journals and proceedings, ten patents/software copyrights, and ten books/monographs with more than 6000 citations and H-index >40. His research interests include satellite navigation, remote sensing, and space/planetary geodesy.

Prof. Jin has been the President of the International Association of Planetary Sciences from 2015 to 2019, the President of the International Association of CPGPS from 2016 to 2017, the Chair of IUGG Union Commission on Planetary Sciences for the period of 2015–2023, the Vice-President of the IAG Commission from 2015 to 2019, the Editor-in-Chief of the *International Journal of Geosciences*, an Editor of *Geoscience Letters*, an Associate Editor for the IEEE TRANSACTIONS ON GEOSCIENCE AND REMOTE SENSING and *Journal of Navigation*, an Editorial Board member of *Remote Sensing*, *GPS Solutions,* and *Journal of Geodynamics*. He was the recipient of the one first-class and four second-class Prizes of Provincial Awards, 100-Talent Program of CAS, Leading Talent of Shanghai, IAG Fellow, IUGG Fellow, Member of Russian Academy of Natural Sciences, Member of European Academy of Sciences, and Member of Academia Europaea.

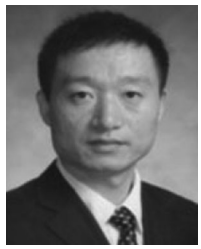

Zhanchuan Cai (Senior Member, IEEE) received the Ph.D. degree from Sun Yat-sen University, Guangzhou, China, in 2007. From 2007 to 2008, he was a Visiting Scholar with the University of Nevada at Las Vegas, NV, USA.

He is currently a Professor with the Faculty of Information Technology, Macau University of Science and Technology, Macau, China, where he is also with the State Key Laboratory of Lunar and Planetary Sciences, Macau University of Science and Technology, Macau, China. His research interests include remote sensing data processing and analysis, intelligent information processing, image processing and computer graphics, and multimedia information security.

He is a member of the ACM, the Chang'e-3 Scientific Data Research and Application Core Team, and the Asia Graphics Association. He is also a Senior Member of the CCF. He was a recipient of the Third prize of the Macau Science and Technology Award-Natural Science Award, in 2012, the BOC Excellent Research Award from the Macau University of Science and Technology, in 2016, and the Third Prize of the Macau Science and Technology Award-Technological Invention Award, in 2018.

Shuo Hu is currently working toward the master's degree in cartography and geography information system with the College of Geoexploration Science and Technology, Jilin University, Changchun, China.

His research interests include application of microwave remote sensing technology in the planetary science and land surface parameters inversion using remote sensing technology.